

## Implantation

### **Annealing of Implanted Layers in (1-100) and (Invited) (11-20) Oriented SiC**

M. Sato

*Hosei University*

### **Codoping of 4H-SiC with N- and P-Donors by Ion Implantation**

M. Laube, G. Pensl

*Universität Erlangen-Nürnberg, Germany*

### **Phosphorus Implantation into 4H-SiC (0001) and (11-20)**

Y. Negoro, N. Miyamoto, T. Kimoto, H. Matsunami

*Kyoto University, Japan*

### **Low Temperature Activation of the Ion-Implanted Dopants in 4H-SiC by Excimer Laser Annealing**

Y. Tanaka, H. Tanoue, K. Arai

*National Institute of Advanced Industrial Science and Technology, Japan*

### **Low-Dose Aluminum and Boron Implants in 4H-and 6H-SiC**

N. S. Saks[1], A. K. Agarwal[2], S. H. Ryu[2], J. W. Palmour[2]

*[1]Naval Research Laboratory, USA; [2]Cree Inc., USA*

### **Comparison of Al and Al/C Co-Implants in 4H-SiC Annealed with an AlN Cap**

K. A. Jones[1], P. B. Shah[1], M. A. Derenge[1], M. H. Ervin[1], G. J. Gerardi[2], J. A. Freitas Jr.[3], G. C. B. Braga[3], R. D. Vispute[4], R. P. Sharma[4], O. W. Holland[5]

*[1]Army Research Lab., USA; [2]William Patterson U., USA; [3]Naval Research Laboratory, USA; [4]University of Maryland, USA; [5]Oak Ridge National Lab., USA*

## Annealing of Implanted Layers in (1 $\bar{1}$ 00) and (11 $\bar{2}$ 0) Oriented SiC

Masataka Satoh\*

*Research Center of Ion Beam Technology, Hosei University,  
Koganei, Tokyo 184-8584, Japan*

Phone; +81-42-387-6091, Fax: +81-42-387-6095, E-mail: mah@ionbeam.hosei.ac.jp

The ion implantation is of importance for the doping of impurities to SiC in the fabrication of the heavily doped region such as source and drain in field-effect-transistor. However, the high-dose ion implantation to (0001)-oriented SiC accompanied by the amorphization leads to a regrowth inducing 3C-SiC crystals during the post-implantation annealing, as shown in Fig. 1. Therefore, the ion implantation to (0001)-oriented SiC has been performed at the elevated sample temperature or at the low dose, which would restrict the device process of SiC.

For the (0001)-oriented SiC, the regrowth of 3C-SiC from the implantation-induced amorphous layer is attributed to the lack of the atomic stacking sequence at the amorphous-crystalline substrate (a/c) interface. For the (1 $\bar{1}$ 00)- and (11 $\bar{2}$ 0)-oriented SiC, however, the atomic stacking sequence of the polytype structure is preserved at the a/c interface even if the amorphous layer is formed by the high-dose implantation. Author and co-workers reported that the implantation-induced amorphous layers on (1 $\bar{1}$ 00)- and (11 $\bar{2}$ 0)-oriented SiC are recrystallized to the original polytype structure according to the underlying substrate during the post-implantation annealing[1-3]. Figure 2 shows Rutherford backscattering (RBS) spectra and the electron diffraction taken from the (1 $\bar{1}$ 00)-oriented 6H-SiC implanted with 100 keV Ar ions at  $2 \times 10^{15}$  /cm<sup>2</sup> at room temperature. RBS spectra reveal that the implantation-induced amorphous layer is recrystallized by annealing at 1000 °C for 5 min. The electron diffraction shows the polytype of the regrown layer is identical to that of the underlying substrate. Also, for the (11 $\bar{2}$ 0)-oriented SiC, the implantation induced amorphous layer is recrystallized to the original structure and the similar results have been obtained for the implantation to 4H-SiC. These results suggest that the high-dose implantation to the (1 $\bar{1}$ 00)- and (11 $\bar{2}$ 0)-oriented SiC can be carried out at room temperature.

The series of spectra shown in Fig. 3 show the reduction in thickness of the amorphous layer as a function of annealing time for the (11 $\bar{2}$ 0)-oriented 6H-SiC at 750 °C[4]. The a/c interface on (11 $\bar{2}$ 0)-oriented 6H-SiC shifts to the surface in equal thickness interval for equal time intervals indicating a uniform regrowth velocity. The regrowth rate at 750 °C is estimated to be 3.5 nm/min. The reduction in thickness of the amorphous layer can be observed by the annealing above 700 °C. The successive decrease of thickness of the amorphous layer indicates that the implantation-induced amorphous layer is epitaxially regrown by annealing above 700 °C. Figure 4 shows the Arrhenius plots of the regrowth rate for (1 $\bar{1}$ 00)-, (11 $\bar{2}$ 0)- and (0001)-oriented 6H-SiC[4,5]. In the case of (0001) SiC, the regrowth rate of 3C-SiC is not uniform. The activation energy of the regrowth rate for the amorphous layer on 6H-SiC is estimated to be 3.4 eV, which is independent to the crystal orientation. The obtained results for the regrowth of the amorphous layer on (1 $\bar{1}$ 00)- and (11 $\bar{2}$ 0)-oriented SiC suggest that the implantation damage can be annealed out at temperatures below 1000 °C.

[1] M. Satoh, K. Okamoto, K. Kuriyama, M. Kanaya, and N. Ohtani, Nucl. Instr. Methods B148 (1999), p. 567.

[2] M. Satoh, Y. Nakaike, K. Uchimura, and K. Kuriyama, Mater. Sci. Forum 338-342 (2000), p. 905.

[3] M. Satoh, Y. Nakaike, and K. Kuriyama, J. Appl. Phys. 89 (2001), p. 61.

[4] M. Satoh, Y. Nakaike, and T. Nakamura, J. Appl. Phys. 89 (2001), p. 1986.

[5] T. Nakamura, S. Matsumoto, and M. Satoh, Abstract of the 13<sup>th</sup> ICCG(Aug. 2001, Kyoto, Japan), p. 217.

\*Temporary address: Purdue University, 1285 EE Building, West Lafayette, IN 47907-1285, U.S.A

satohm@ecn.purdue.edu

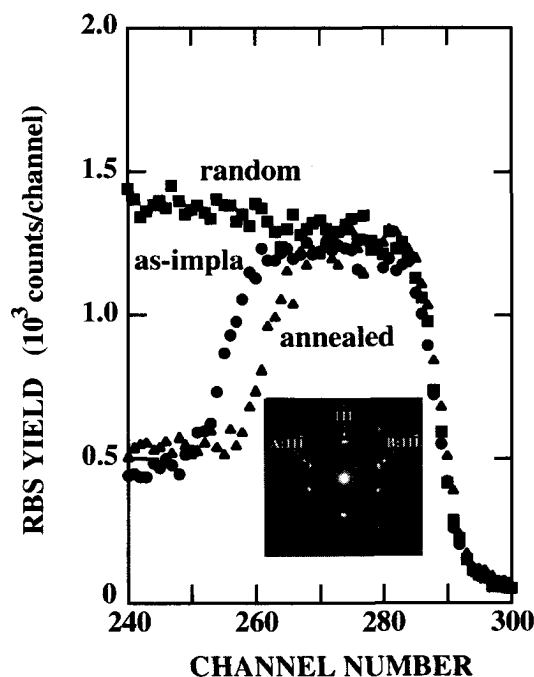


Fig. 1: RBS spectra taken from the 100 keV Ar ( $2 \times 10^{15}/\text{cm}^2$ ) implanted 6H-SiC(0001) before and after annealing at 950 °C for 30 min. The electron diffraction shows that the amorphous layer is recrystallized to 3C-SiC.

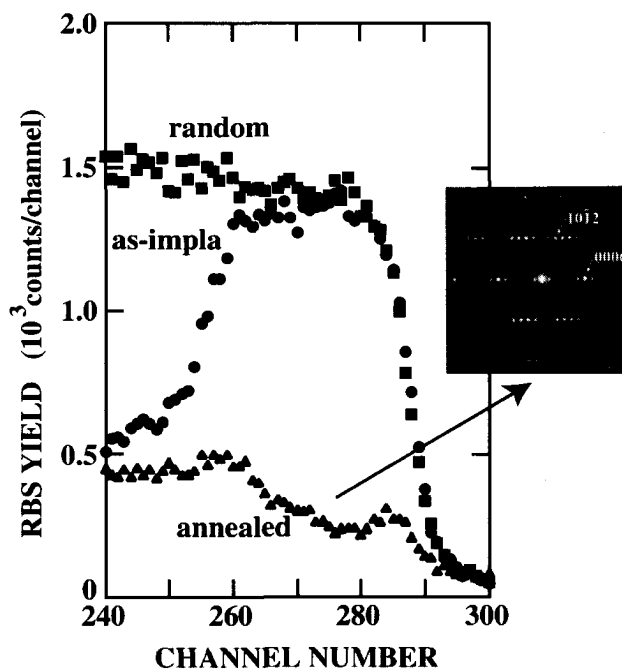


Fig. 2: RBS spectra take from 100 keV Ar ( $2 \times 10^{15}/\text{cm}^2$ ) implanted 6H-SiC(1-100) before and after annealing at 1000 °C for 5 min. The electron diffraction shows that the regrown layer is 6H-SiC.

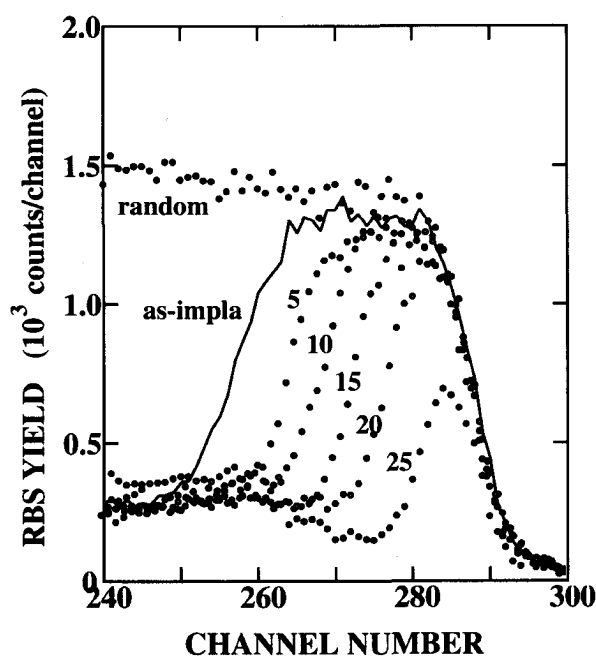


Fig. 3: RBS spectra taken from 100 keV Ar ( $2 \times 10^{15}/\text{cm}^2$ ) implanted 6H-SiC(11-20) as a function of annealing time at 750 °C. The numbers in figure represent the annealing time in minutes.

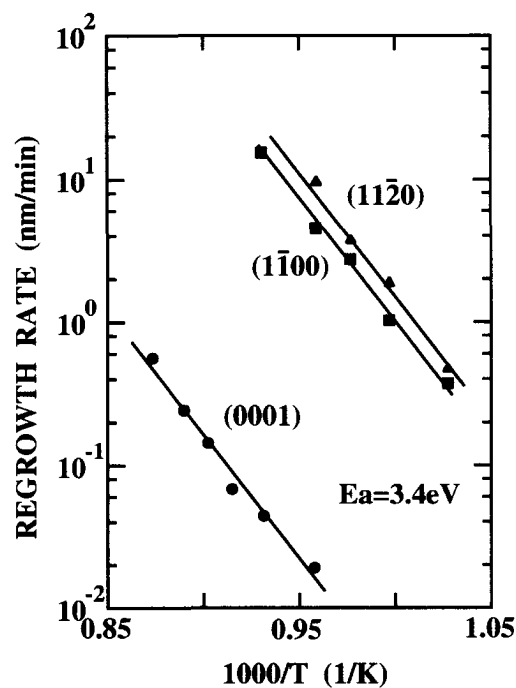


Fig. 4: Arrhenius plots of the regrowth rate of the amorphous layer in 6H-SiC. The amorphous layer on 6H-SiC(0001) is recrystallized to 3C-SiC.

## Codoping of 4H-SiC with N- and P-Donors by Ion Implantation

M. Laube, G. Pensl

Institute of Applied Physics, University of Erlangen-Nürnberg, Staudtstrasse 7,  
D-91058 Erlangen, Germany, phone: +49 9131 852 8426, fax: +49 9131 852 8423,  
e-mail: gerhard.pensl@physik.uni-erlangen.de

In order to reduce the series resistance in SiC-based power devices, highly doped areas are required. In the case of n-type SiC, usually nitrogen (N) atoms residing at carbon lattice sites [1] are employed as the dominating donor. For N concentrations  $[N]$  greater than  $2 \times 10^{19} \text{ cm}^{-3}$ , the incorporated N atoms start to form partially electrically inactive centers (probably precipitates) and, in addition, such SiC wafers show a high internal tension and become easily brittle.

One possible way to increase the conductivity in n-type SiC and to simultaneously avoid the drawbacks of high N concentrations - as described above - is the codoping of SiC by nitrogen and phosphorus (P). P atoms also act as donors residing, however, at Si lattice sites [2]. They have an ionization energy which is close to the ionization energy of N donors [3, 4].

In this paper, we successfully demonstrate codoping by implantation of N and P. Identical box profiles of N and P to a depth of  $1.3 \mu\text{m}$  are generated by multiple implantation. We have implanted two sets of p-type 4H-SiC epilayers ( $N_{\text{Al}}-N_{\text{comp}} = 4 \times 10^{16} \text{ cm}^{-3}$ ) with different mean donor concentrations:

Implantation 1 :  $[N] = [P] = 1 \times 10^{18} \text{ cm}^{-3}$  / Implantation 2 :  $[N] = [P] = 2 \times 10^{19} \text{ cm}^{-3}$

Each set consists of sample a), sample b) and sample c) implanted with N, P and (N+P), respectively. All the samples have been annealed in a SiC container at  $1700^\circ\text{C}$  for 30 min resulting in a complete electrical activation of implanted ions. The parameters of implanted donors have been determined by Hall effect investigations in van der Pauw arrangement. In order to avoid leakage currents over the implanted n-p junction, mesa structures have been fabricated by reactive ion etching. Results of the Hall effect analysis are summarized in Table I and partially revealed in Figs. 1 and 2; the main features are:

1. The total implanted concentration  $[N+P]$  is electrically active.
2. Implantation 1 and 2 (samples c)) result in low resistivities of  $0.05 \Omega\text{cm}$  and  $0.014 \Omega\text{cm}$ , respectively, at 300K.
3. At identical implanted concentration, the Hall mobility in P-implanted layers is higher than in N-implanted layers in the temperature range from 80K to 400K (not shown here).

Hot N/P-coimplanted samples at total mean concentrations of  $[N+P] > 10^{20} \text{ cm}^{-3}$  are in process, the corresponding Hall effect results will be compared with those, which are taken on layers only implanted with N at identical concentrations.

### References

- [1] H. H. Woodbury, G. W. Ludwig, Phys. Rev. **124** (1961), p. 1083.
- [2] S. Greulich-Weber, M. Feege, J. M. Spaeth, E. N. Kalabukhova, S. N. Lukin, E. N. Mokhov, Solid State Commun. **93** (1995), p. 393.
- [3] T. Troffer, C. Peppermüller, G. Pensl, A. Schöner, J. Appl. Phys. **80** (1996), p. 3739.
- [4] M. A. Capano, J. A. Cooper, Jr., M. R. Melloch, A. Saxler, W. C. Mitchel, Mater. Sci. Forum **338-342** (2000), p. 703.

Table I.

Donor parameters determined by fit of the neutrality equation to the measured Hall effect data taken on (N+P)-coimplanted samples c).  $\Delta E(h)$ ,  $\Delta E(k)$  denote the ionization energy of donors residing at hexagonal (h) or cubic (k) lattice site.  $N_D(h/k)$  denotes the total donor concentration.  $\rho$  and  $\mu_{H,e}$  are the room-temperature (RT) values of resistivity and electron Hall mobility, respectively.

Hall effect parameter	Implantation 1 sample c)	Implantation 2 sample c)
$\Delta E(h)$ (meV)	59	26
$\Delta E(k)$ (meV)	103	
$N_D(h/k)$ ( $\text{cm}^{-3}$ )	$1.9 \times 10^{18}$	$4.3 \times 10^{19}$
$\rho$ at RT ( $\Omega\text{cm}$ )	0.05	0.014
$\mu_{H,e}$ at RT ( $\text{cm}^2/\text{Vs}$ )	170	42

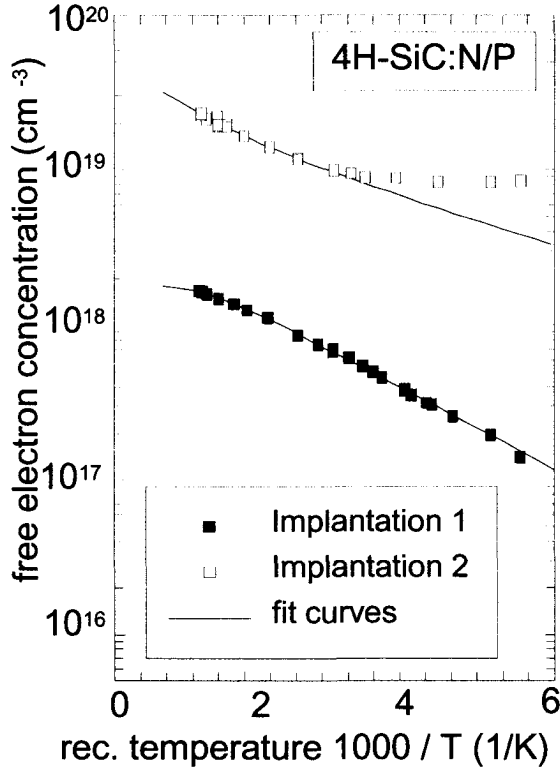


Fig. 1. Free electron concentration as a function of the reciprocal temperature obtained from Hall effect measurements on the (N+P)-codoped samples c). Symbols represent the experimental data (filled squares: implantation 1, open squares: implantation 2). The solid lines correspond to a least-squares-fit of the neutrality equation to the experimental data. The fit parameters are given in Table I.

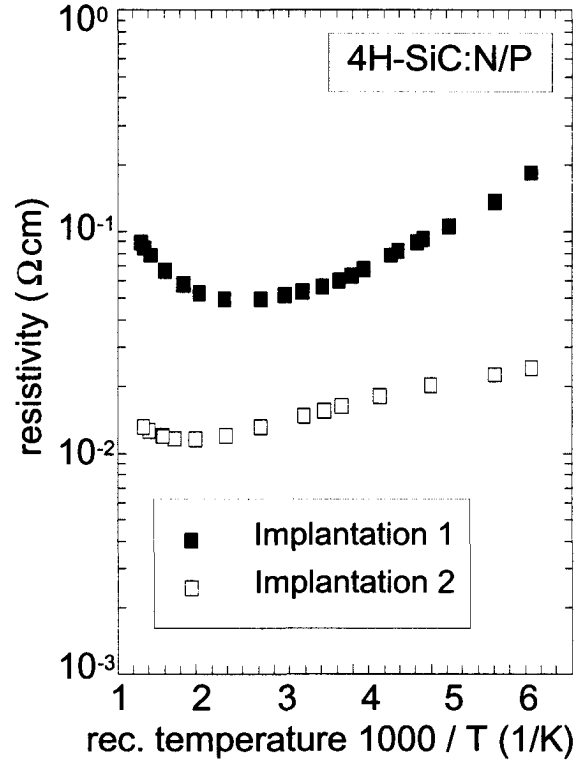


Fig. 2. Resistivity as a function of the reciprocal temperature. Filled squares correspond to implantation 1 sample c), open squares to implantation 2 sample c).

## Phosphorus Implantation into 4H-SiC (0001) and (11 $\bar{2}$ 0)

Y. Negoro, N. Miyamoto, T. Kimoto, and H. Matsunami

*Department of Electronic Science and Engineering, Kyoto University,  
Yoshidahonmachi, Sakyo, Kyoto 606-8501, Japan*

Tel: +81-75-753-5341, Fax: +81-75-753-5342, e-mail: negoro@mitsunami.kuee.kyoto-u.ac.jp

To form selective n<sup>+</sup> regions in SiC, phosphorus ion (P<sup>+</sup>) and nitrogen ion (N<sup>+</sup>) implantation are commonly employed. Recently P<sup>+</sup> implantation, instead of N<sup>+</sup> implantation, has attracted increasing attention to obtain lower sheet resistances. P<sup>+</sup> implantation at an elevated temperature followed by annealing at a high temperature above 1600 °C is effective to reduce sheet resistances [1, 2]. However, a recent report has shown that when activation annealing is performed at a high temperature in Ar, considerable roughening and macrostep formation is observed [3]. To establish a similar process in Si technology, the major challenges include successful implantation at RT, the reduction of annealing temperature, and keeping surface flatness during annealing processes. In this work, the authors demonstrate that SiC (11 $\bar{2}$ 0) may be a solution to meet these requirements.

P-type 4H-SiC (0001) and (11 $\bar{2}$ 0) epilayers with an acceptor concentration of 1~5×10<sup>16</sup> cm<sup>-3</sup> grown in the authors' group were used in this study. Multiple implantation of P<sup>+</sup> was carried out to obtain a 0.25 μm-deep box profile of P (10~180 keV, total dose: 4×10<sup>15</sup> cm<sup>-2</sup>) or a 0.45 μm-deep box profile of P (10~360 keV, total dose: 1×10<sup>16</sup> cm<sup>-2</sup>). The implantation temperature was RT or 800 °C. Post-implantation annealing was performed at 1100~1700 °C for 30 min in Ar ambience. The electrical properties of implanted regions were characterized by Hall effect measurements using the van der Pauw configuration at RT. The implantation-induced damage was analyzed by RBS channeling measurements with a 2.0 MeV He<sup>2+</sup> primary beam.

Figure 1 (a) shows the aligned spectra of as-implanted and 1700 °C-annealed 4H-SiC (0001) samples. The aligned yields of the damaged region (channel number: 230-280) are close to the random yields in the case of RT-implantation without annealing. Although the yields decrease by annealing at 1700 °C, severe damages near the surface still remain. In contrast, the damage is considerably decreased for a 800 °C-implanted and 1700 °C-annealed sample. Figure 1 (b) shows the aligned spectra of 4H-SiC (11 $\bar{2}$ 0) samples implanted at RT followed by annealing at 1700 °C. The figure demonstrates that implantation-induced damages are reduced down to the virgin (unimplanted) level even with RT-implantation followed by annealing at 1700 °C. This indicates that significantly better lattice recovery is realized in 4H-SiC (11 $\bar{2}$ 0) than (0001), owing to a much faster recrystallization rate along the <11 $\bar{2}$ 0> direction [4]. Thus, 4H-SiC (11 $\bar{2}$ 0) may possess much potential to reduce implantation and annealing temperature.

Figure 2 shows an AFM image of RT-implanted and 1300 °C-annealed 4H-SiC (11 $\bar{2}$ 0) sample. The surface exhibits a smooth surface as observed even by an AFM. The surface was mirror-like, and the value of root-mean-square (Rms) surface roughness was as low as 1.5 nm (10×10 μm<sup>2</sup>).

Figure 3 shows the measured sheet resistance of  $P^+$ -implanted regions as a function of annealing temperature. In the case of 800 °C-implantation into 4H-SiC (11 $\bar{2}$ 0), the sheet resistance takes a minimum value of 27  $\Omega/\square$  at an annealing temperature of 1700 °C. This is the lowest value ever reported. RT-implantation into (11 $\bar{2}$ 0) resulted in significantly lower sheet resistances compared to RT-implantation into (0001). A reasonable sheet resistance of 460  $\Omega/\square$  was obtained even by RT-implantation followed by 1300 °C-annealing, when (11 $\bar{2}$ 0) was employed. This may bring considerable improvement in SiC device processing technology as well as device performance.

- [1] M. A. Capano et al., J. Electron. Mat., **29**, 210 (2000).
- [2] S. Imai et al., Mat. Sci. Forum, **338-342**, 861 (2000).
- [3] M. A. Capano et al., J. Electron. Mat., **28**, 214 (1999).
- [4] M. Satoh et al., Mat. Sci. Forum, **338-342**, 905 (2000).

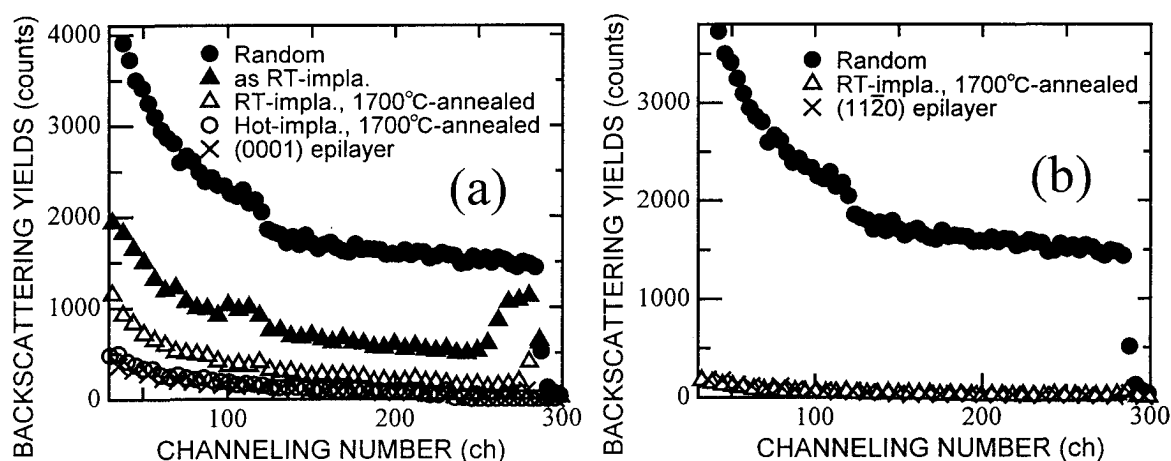


Fig. 1. RBS spectra of 4H-SiC layers before and after annealing.  $P^+$  implantation was done with a total dose of  $4 \times 10^{15} \text{ cm}^{-2}$  at RT and 800 °C: (a) 4H-SiC (0001), (b) 4H-SiC (11 $\bar{2}$ 0). The spectrum of a virgin sample is also shown as reference.

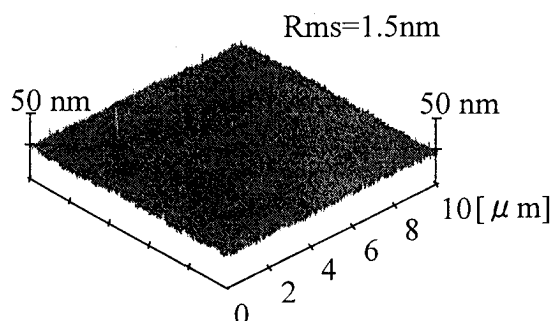


Fig. 2. AFM image of RT-implanted and 1300 °C-annealed 4H-SiC (11 $\bar{2}$ 0).

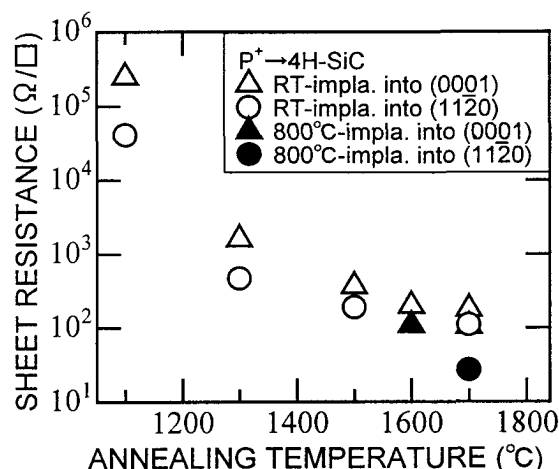


Fig. 3. Dependence of sheet resistance on annealing temperature of  $P^+$ -implanted 4H-SiC (0001) and (11 $\bar{2}$ 0).

## Low temperature activation of the ion-implanted dopants in 4H-SiC by excimer laser annealing

Yasunori Tanaka<sup>1</sup>, Hisao Tanoue<sup>2</sup> and Kazuo Arai<sup>1</sup>

<sup>1</sup>Research Center of Power Electronics

<sup>2</sup>Nanoelectronics Research Institute

National Institute of Advanced Industrial Science and Technology (AIST)

1-1-1 Umezono, Tsukuba, Ibaraki 305-8568, Japan

Tel. +81-298-61-5691, Fax. +81-298-61-3397

E-mail: yasunori-tanaka@aist.go.jp

Annealing process at extremely high temperature ( $>1500^{\circ}\text{C}$ ) for the activation of the ion-implanted dopants in SiC causes some serious problems, e.g. the evaporation of the surface atoms and the redistribution of the ion-implanted dopants. Therefore it has been expected that a new annealing process at low temperature below  $1000^{\circ}\text{C}$  will be developed. Excimer laser annealing will be a very hopeful technique to activate the ion-implanted dopants in SiC at low temperature. Although several groups[1],[2] reported the effect of the laser annealing of the ion-implanted SiC, there was a little description of the electrical property. Hishida et al.[3] reported the effect of the excimer laser annealing(XeCl) in  $\text{Al}^{+}$  and  $\text{N}^{+}$  implanted 6H-SiC. However, in their study the activation efficiencies in both cases were too low to apply the laser annealing to SiC device process instead of the furnace annealing. In this study, by the improvement of the condition of the ion implantation and the excimer laser irradiation we succeeded to achieve extremely high activation efficiency of phosphorus( $\text{P}^{+}$ ) ion-implanted 4H-SiC at low temperature as  $\sim 800^{\circ}\text{C}$ .

In this study we used 4H-SiC(0001) wafer with epitaxial layer (p-type,  $\text{N}_a\text{-N}_d \sim 5.0 \times 10^{15}/\text{cm}^3$ , Si-face,  $8^{\circ}$  off,  $5\mu\text{m}$  thickness) purchased from Cree Research Inc. and cut them into  $4 \times 4\text{mm}^2$  for the  $\text{P}^{+}$  ion implantation. To make a box profile layer we performed the multiple energy ion implantation in the energy range of 30-100keV with the total dose of  $5.7 \times 10^{15}/\text{cm}^2$ . The substrate was heated at  $500^{\circ}\text{C}$  during the ion implantation in order to prevent the amorphization of the implanted layer. The implanted sample was irradiated by XeCl excimer laser ( $\lambda=308\text{nm}$ ) in ultra high vacuum chamber( $3.0 \times 10^{-7}\text{Torr}$ ). The laser irradiation was carried out by 4 steps as shown in Table 1. By using this “step irradiation” method the photon energy is effectively provided to the ion-implanted layer without surface evaporation. During the laser irradiation the substrate was heated from room temperature to  $800^{\circ}\text{C}$  to investigate the combination effect of the laser annealing and the thermal annealing.

Figure 1 shows the substrate temperature dependence of the free electron concentration and sheet resistance of the laser annealed samples. Those of the furnace annealed sample at  $1600^{\circ}\text{C}$  for 5min in Ar ambient are also shown in this figure. Although the implanted phosphorus was electrically activated even at room temperature, the free electron concentration is considerably lower than that of the furnace annealed sample. The free electron concentration, however, abruptly increases above  $500^{\circ}\text{C}$  and reaches  $2.95 \times 10^{20}/\text{cm}^3$  at  $800^{\circ}\text{C}$  which corresponds to three times as much as that of the furnace annealed sample. At the same temperature sheet resistance is  $164.7\Omega/\square$  enough to use for the source or drain



	step 1	step 2	step 3	step 4	total
Energy density [ $\text{J}/\text{cm}^2$ ]	0.8	1	1.2	1.3	
shots	600	600	600	600	2400

Table 1 Condition of the excimer laser irradiation : the excimer laser was irradiated on the implanted sample by 4 steps from low to high energy density.

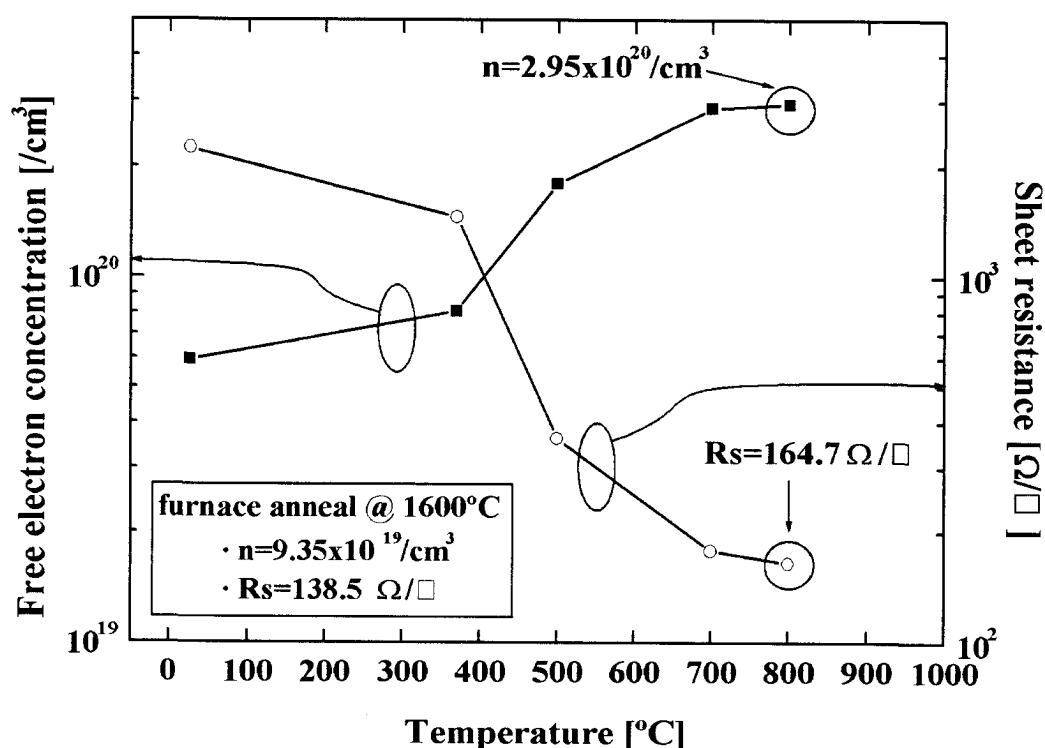


Figure 1 Substrate temperature dependence of the free electron concentration and sheet resistance of the laser annealed samples. Those of the furnace annealed sample are also shown in this figure.

region in SiC-MOSFET or MESFET. The further reduction of sheet resistance will be expected by optimizing the condition. From the results of SIMS and AFM there are no redistribution of the dopants and no surface roughness that is observed in the furnace annealed sample. In the presentation I will also talk about the electrical property of pn-junction fabricated by the laser annealing.

## Reference

- [1] S.D. Russell and A.D. Ramirez, Appl. Phys. Lett., **74**, 3368 (1999).
- [2] S. Ahmed, C.J. Barbero and T.W. Sigmon, Appl. Phys. Lett., **66**, 712 (1997).
- [3] Y. Hishida, M. Watanabe, K. Nakashima and O. Eryu, Material Science Forum, **338-342**, 873 (2000).

## Low-Dose aluminum and boron implants in 4H- and 6H-SiC

N. S. Saks<sup>1</sup>, A. K. Agarwal<sup>2</sup>, S-H. Ryu<sup>2</sup>, and J.W. Palmour<sup>2</sup>

<sup>1</sup> Naval Research Laboratory, Code 6813, Washington, D.C. 20375 USA.

(202) 767-2534, (202) 404-7194 (fax), [saks@nrl.navy.mil](mailto:saks@nrl.navy.mil)

<sup>2</sup> Cree, Inc., 4600 Silicon Drive, Durham, NC 27703, USA.

Due to the difficulty of fabricating doped layers in SiC by diffusion, doping of SiC by implantation has been studied extensively. To date, most research on n- and p-type implants has concentrated on heavily doped layers suitable for transistor source/drain regions, ohmic contacts, etc. [1]. Here we report on boron and aluminum p-type implants in 4H- and 6H-SiC at low doses suitable for active regions in SiC power devices.

For this work two main types of samples have been fabricated: (a) MOS capacitors, fabricated on p-type SiC substrates, used to obtain depth profiles of the activated acceptor concentrations, and (b) Hall bars, fabricated on n-type substrates, used to obtain free hole densities and hole mobilities as a function of temperature. In addition, samples from the same wafers were obtained for SIMS measurements of implanted profiles and for AFM studies of surface roughness. Multiple-energy implants were performed on heated substrates to obtain “box” profiles with doping densities of  $\sim 1 \times 10^{17} / \text{cm}^3$  and  $\sim 0.5 \mu\text{m}$  thick. Anneals at 1300-1500°C were performed in an argon ambient, while anneals at 1600°C were performed in a silicon-overpressure ambient.

Due to limited space, we present here a few selected (mostly 4H) experimental results:

- The best results for surface roughness ( $< 0.3 \text{ nm rms}$ ) were obtained using a si-overpressure ambient at 1600°C, independent of the type of implant or the SiC polytype.
- SIMS results show good correlation between implanted B profiles and simulations (Fig. 1) at all anneal temperatures. Some depletion of the boron is clearly observed at the surface.
- Excellent, uniform activation of implanted Al is observed for anneal temperatures  $\geq 1400^\circ\text{C}$  (Fig. 2). The calculated activation rate is  $\sim 75\%$  (4H-SiC). Despite this high activation rate, high quality layers are not produced in 4H for anneals below 1600°C (see Fig. 4). Poor activation is obtained at 1300°C.
- Activation of implanted boron is much smaller (at  $\sim 10\text{-}20\%$ ) compared to Al, as is well-known. Surprisingly, however, the activation rates appear to depend on position (Fig. 3). Peaks in the activated boron correlate with the implant peaks for each implant energy.
- Hall measurements have been made over a wide temperature range (150K - 400°C) in order to determine free hole densities and hole mobilities in the implanted layers. Free hole density is shown as a function of inverse temperature in Fig. 4. From these data and standard models [1], it is possible to extract the true density of activated acceptors and the levels of compensation (which presumably arise from un-annealed implant damage). For example, from the fit of the model to the data in Fig. 4, within experimental accuracy,  $\sim 100\%$  of the implanted Al ions are activated. However, about 25% of the doping is compensated with deep donors even for the highest anneal temperature (1600°C). The level of compensation is much higher for anneal temperatures at or below 1500°C, implying that anneal temperatures of  $\sim 1600^\circ\text{C}$  or higher are necessary to produce near-device-quality layers.
- Hole mobilities have been measured as a function of temperature for both B and Al implants.

Mobilities close to bulk values are observed at  $T \geq 400\text{K}$ . At  $200 \leq T \leq 400\text{K}$ , hole mobilities are considerably reduced compared to bulk, probably due to scattering from charged compensating defects. Interestingly, hole mobilities in B-implanted layers are up to 30% higher compared to Al-implanted layers at low temperatures ( $\sim 250\text{K}$ ), suggesting that there are fewer compensating defects in B-implanted layers.

In summary, device-quality, lightly doped p-type layers can be fabricated by B- and Al-implantation using Si-overpressure annealing at  $1600^\circ\text{C}$  for both 4H- and 6H-SiC. Aluminum implants would be preferred when a known doping profile is required, e.g., for the p-well of a DMOS power FET [2], due to the low post-implant diffusion and high activation of Al. On the other hand, higher quality layers, with higher hole mobility and reduced compensation, are obtained with boron implantation, which may be preferable for other applications.

Acknowledgement: This work was partially supported by Dr. G. Campisi of ONR.

[1] T. Troffer, M. Schadt, T. Frank, H. Itoh, G. Pensl, J. Heindl, H.P. Strunk, and M. Maier, Phys. Stat. Sol. A **162**, p. 277 (1997).

[2] A. Agarwal, S-H. Ryu, M. Das, L. Lipkin, J. Palmour, and N. Saks, 13<sup>th</sup> Int. Symp. on Power Semiconductor Dev. and ICs, Osaka, Japan, June 4-7, 2001.

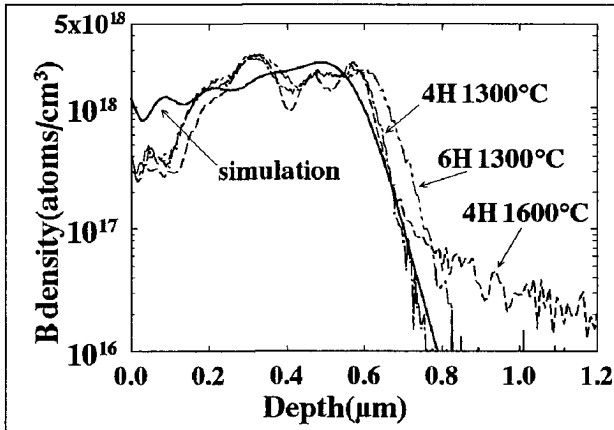


Fig. 1: SIMS profile of Al implants in 4H- and 6H-SiC vs. anneal temperature.

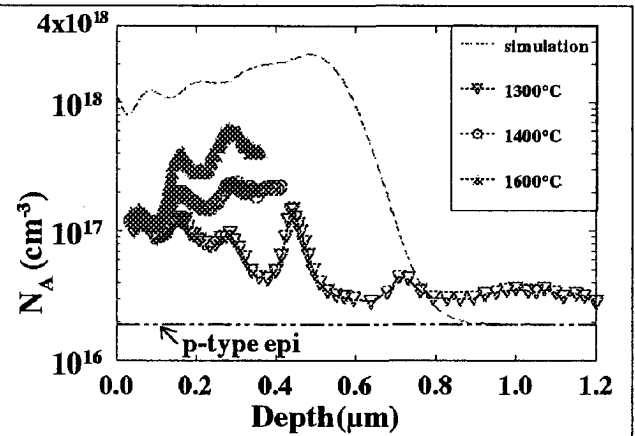


Fig. 3: Depth profile of activated implanted B acceptors vs. anneal temperature.

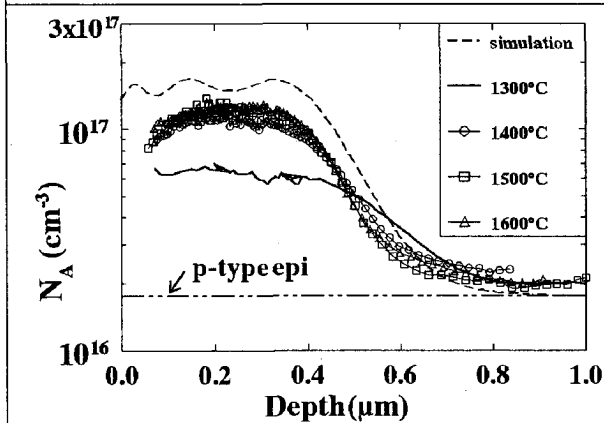


Fig. 2: Depth profile of activated Al acceptors vs. anneal temperature (from C-V).

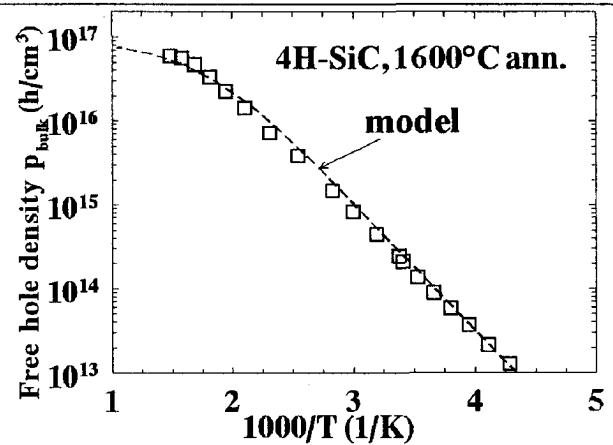


Fig. 4: Comparison of free hole density in Al-implanted layer to theoretical model.

### **Comparison of Al and Al/C Co-Implants in 4H-SiC Annealed with an AlN Cap**

K.A. Jones, P.B. Shah, M.A. Derenge, and M.H. Ervin

P: (301) 394-2005, F: (301) 394-4562, kajones@arl.army.mil

Army Research Lab, 2800 Powder Mill Road, Adelphi, MD 20783

G.J. Gerardi

William Patterson U., Chemistry & Physics Dept., Wayne, NJ, 07470

J. A. Freitas Jr. and G.C.B. Braga

Naval Research Laboratory, Code 6877, 4555 Overlook Ave., Washington, D.C. 20375

R.D. Vispute and R.P. Sharma

University of Maryland, Physics Dept., College Park, MD 20742

O.W. Holland

Oak Ridge National Lab, Oak Ridge, TN 37831

Implants into SiC can be activated only at temperatures at which silicon also preferentially evaporates at detectable rates and modifies the surface region - the region that is often being probed. The problem is most severe when the samples are annealed in a vacuum or in argon, but even when the samples are annealed in a silane over pressure or in the presence of SiC powder, silicon evaporates at the same rate; only the silicon deposition rate increases. The process of recovery and evaporation go on simultaneously, and one affects the other so the state of activation is determined by the annealing atmosphere as well as the time and temperature. Also, the evaporation will completely dominate the process unless severe limits are placed on the annealing times and temperatures that can be used. This greatly limits the range of times and temperatures that can be studied.

We have developed a method that impedes the evaporation of silicon by using an AlN cap that is stable up to  $\sim 1600^\circ\text{C}$ , does not react with the SiC, and can be removed preferentially with a KOH etch. Not only does this enable us to minimize the effects of silicon out-diffusion, we can also use higher temperatures for longer times which allows the sample to more closely approach its equilibrium state. In this paper we examine and compare how annealing 4H-SiC box implanted to a depth of  $0.3\ \mu\text{m}$  with  $10^{20}\ \text{cm}^{-3}$  Al or co-implanted with  $10^{20}\ \text{cm}^{-3}$  Al and  $10^{20}\ \text{cm}^{-3}$  C between  $1300$  and  $1700^\circ\text{C}$  affects the electrical and optical properties of the material. This is done by measuring the sheet resistance as a function of temperature, recording the electron paramagnetic (EPR) spectra, and examining the low temperature cathodoluminescence (CL) spectra.

The log of the sheet resistance versus annealing temperature plots in Fig. 1, show that the implants do start to become electrically activated at annealing temperatures  $\sim 1400^\circ\text{C}$ . The percent activation in the co-implanted sample is significantly larger after the  $1400$  and  $1500^\circ\text{C}$  anneal compared to the Al implant. However, the resistance of the co-implanted sample is higher after the  $1600^\circ\text{C}$  anneal than it is after the  $1500^\circ\text{C}$  anneal, whereas the resistance of the Al implanted material continues to decrease as the annealing temperature increases, and it is now lower than that of the co-implanted sample.

This suggests that some of the Al dopants in the co-implanted material have ceased to be electrically active as the material more closely approaches its equilibrium configuration. One explanation is that the solubility of Al in the more C rich region is smaller and that some of the Al has precipitated out, possibly as  $\text{Al}_4\text{SiC}_4$ . We show that this explanation is consistent with dilute solution theory as Al is less soluble in C than it

is in Si due, in part, to the strong Al - C bonds. The greater degree of electrical activation in the co-implanted sample at the lower annealing temperatures can be explained by a smaller activation energy required to form a precipitate than to occupy a Si site in a solid solution. This implies that the Al can be an electrically active dopant when it is in an activated complex as it moves from its as-implanted state towards its equilibrium position.

That the Al atoms are "in transit" to their equilibrium positions is supported by the observation that the  $\text{Al}_{\text{Si}}$  EPR signal is not detected in either type of sample even after the 1600°C anneal. We estimate that we would be able to detect this signal near 2777 G if only 1% of the Al atoms were at equilibrium Si sites. Rather, a broad signal centered near 3100 G is observed in some samples. Interestingly, the signal is detected at different annealing temperatures for the two types of samples. It is observed in the as-implanted Al doped sample, as well as in the Al doped samples annealed at 1300 and 1500°C. In the co-implanted samples this signal was detected in the wafers annealed at 1400 and 1600°C. There is virtually no anisotropy in this signal suggesting that the paramagnetic defect centers responsible for it are not strongly bonded to the crystal lattice.

This annealing technique also enables one to obtain well defined CL spectra to complement the paucity of data on the 4H polytype as most of the data in the literature is for 6H-SiC. Examples are the 5 and 10 KeV spectra for the Al implanted sample annealed at 1300°C shown in Fig.2. In addition to the pair of  $\text{D}_{\text{I}}$  peaks near 2.9 eV and the  $\text{D}_{\text{II}}$  peak near 3.2 eV and its phonon replicas between 3.2 and 3.05 eV, there are peaks near 3.0, 3.25 and 3.35 eV. One of the many interesting trends we observe is that the height of the higher energy peak in the doublet near 2.9 eV increases with the annealing temperature, and for the same annealing temperature its relative height is larger in the co-implanted samples. Because each peak is thought to be associated with inequivalent atomic sites, one can possibly decipher what sites they are by learning what is happening during the annealing process.

We should soon be able to shed more light on what these processes are as we have recently learned how to anneal wafers at 1700°C by capping the AlN cap with an  $\text{Al}_2\text{O}_3$  cap. We expect to have the electrical and optical data for samples annealed at this temperature by the time of the meeting. RBS is also being done on these samples.

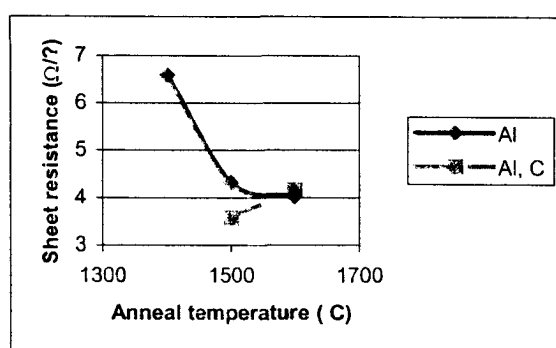


**Fig. 1.** Sheet resistance of Al and Al, C co-implanted samples plotted as a function of their annealing temperatures.

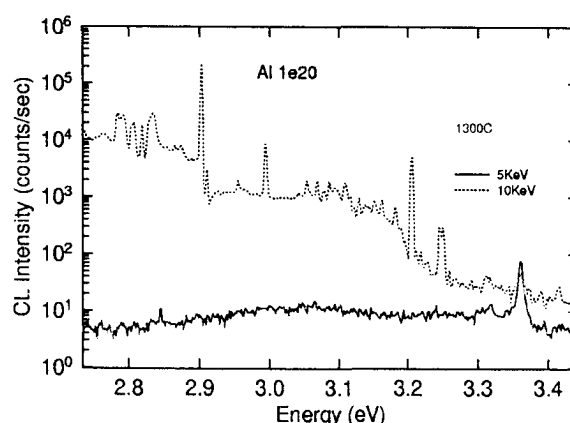


**Fig. 2.** 5 and 10 KeV CL spectra of the Al implanted sample annealed at 1300°C.